Electronic supplementary information

Accurate construction of hierarchical nickel-cobalt oxide multishell yolk-shell structure with large and ultrafast lithium storage capability

Jin Leng,[a] Zhixing Wang, [a] Xinhai Li,[a] Huajun Guo,[a] Hangkong Li,[b] Kaimin Shih,[b] Guochun Yan, [a,c] and Jiexi Wang*[a]

[a]*School of Metallurgy & Environment, Central South University, Changsha 410083, P. R. China.*

[b]*Department of Civil Engineering, The University of Hong Kong, Hong Kong*

[c]*Chimie du Solide-Energie, UMR 8260, College de France, 11 Place Marcelin Berthelot, 75231, Paris, Cedex 05, France*

Prepared for submission to *Journal of Materials Chemistry A*

April 5th， 2017

*Corresponding authors.

E-mail addresses: wangjiexikeen@csu.edu.cn (J. Wang).

Part I: Experimental Section

Material preparation

Multishell yolk-shell structured nickel-cobalt oxide microspheres were prepared by one-pot spray pyrolysis. A diagram of the spray pyrolysis equipment is shown in Figure S1. Firstly, the transition metal nitrates [$Co(NO_3)_2 \cdot 6H_2O$ and $Ni(NO_3)_2 \cdot 6H_2O$] were dissolved in distilled water with a Ni/Co mole ratio of 1:2. PVP was then dissolved in 200 ml of the prepared precursor solution. The amount of PVP dissolved in the solution was varied from 0 to 10 g. After that, a large number of droplets were generated from the above solution by a 1.7 MHz ultrasonic atomizer (Model NB-150U). Then, these droplets were fed into a 3-zone vertical furnace reactor with diameter of 100 mm and length of 1500 mm. The as-prepared powders were collected using an electrostatic precipitator. The operating temperature was increased from 500°C to 800°C.

Material characterization

The morphology and microstructure of the microspheres were characterized by scanning electron microscopy (SEM, JSM-5612LV) and high-resolution transmission electron microscopy (TEM, Tecnai G12, 200 kV). X-ray diffractometer (XRD, Rint-2000, Japan) with Cu-Kα radiation (λ = 1.5418 Å) was used to investigate the crystal structures of the prepared powder particles. The specific surface area of the as-prepared microspheres was determined by the method of Brunauer–Emmett–Teller (BET, ASAP 2020 M). The pore size distribution was obtained from the N_2 adsorption branch. Thermogravimetric analysis (TGA, SDT Q600) was performed to study the thermal stability of the as-obtained particles.

Electrochemical measurement

The electrochemical properties of the resulting materials were investigated by a CR2025 coin-type cell with lithium foil serving as counter electrode and reference electrode. The working electrode was assembled by coating electrode slurry, consisting of fully mixed nickel-cobalt oxide microspheres (70 wt%) as active materials, acetylene black (15 wt%) as conductive agent and polyvinylidene fluoride (PVDF) (15 wt%) as binder, onto copper foils and drying overnight at 120°C. A porous polypropylene film was used as separator. The electrolyte was composed of 1 M $LiPF_6$ dissolved in a mixed organic solvent of ethylene carbonate (EC), ethyl methyl carbonate (EMC), and dimethyl carbonate (DMC) (1:1:1 in volume). The coin-type cells were assembled in an Ar-filled glove box.

Charge–discharge tests of the materials were performed through cycling in a potential window between 3.0 and 0.01 V at various fixed current densities. Cyclic voltammetry (CV) was carried out with a CHI 660A electrochemical analyzer in the voltage range of 0.01 to 3 V at a scan rate of 0.1 mV s^{-1}. Electrochemical impedance spectroscopy (EIS) measurements of the samples were conducted using a CHI 660D electrochemical analyzer in the frequency range from 0.01 Hz to 100 kHz.

Part II: Supporting Figures and Tables

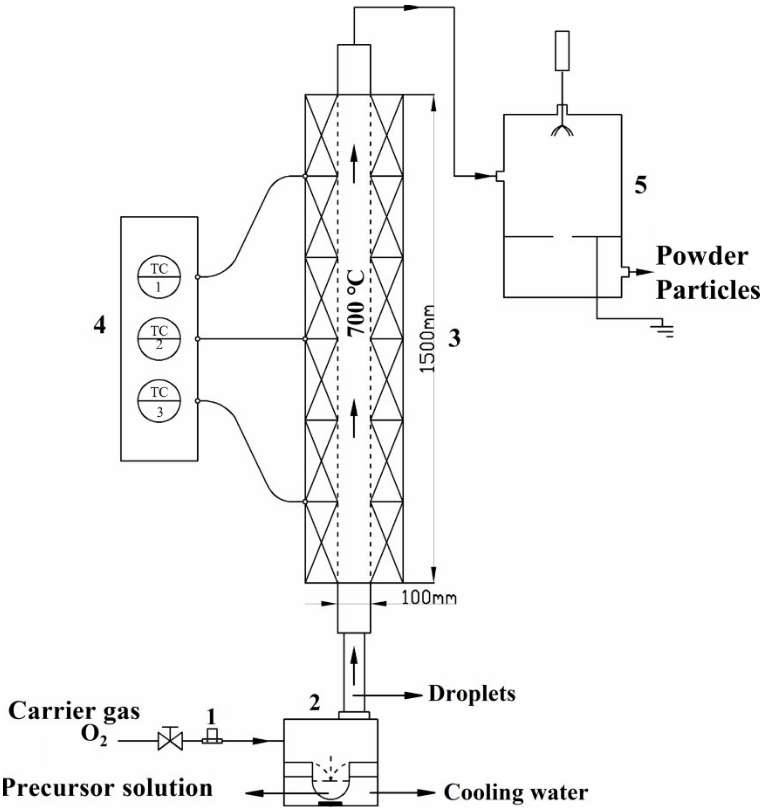

Figure S1 A schematic of the apparatus and reaction mechanism for spray pyrolysis in this study: (1) flow meter; (2) ultrasonic nebulizer; (3) 3-zone vertical furnace reactor; (4) temperature control panel; (5) electrostatic precipitator.

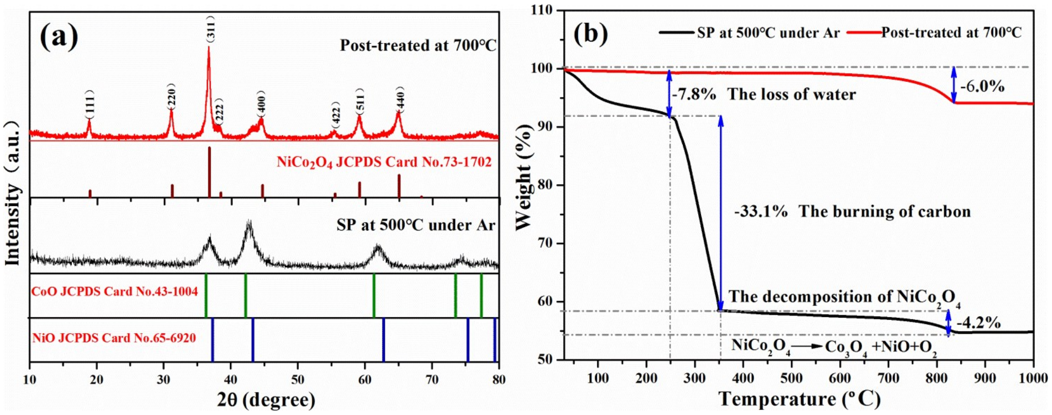

Figure S2 XRD patterns and TG curves of the powder particles directly synthesized at 500 °C under Ar atmosphere and the as-prepared particles heat-treated at 700°C: a) XRD patterns, b) TG curves.

The XRD pattern of the precursor particles (Figure S2a) consists of a few broad peaks indexed to NiO and CoO phases. While the XRD pattern of the sample after heat treatment under O_2 atmosphere (Figure S2a) exhibits a high crystallinity indexed to major $NiCo_2O_4$ with a minor NiO phase[1-3], which is the same as the XRD pattern of the particle (Figure S5a) directly prepared by one-pot SP with PVP at 700°C under O_2 atmosphere. The weight loss between 250°C and 350°C of the TG curve of the precursor microspheres (Figure S2b) further identified the existence of carbon[4, 5]. No weight loss of carbon in the TG curve indicates the carbon have been completely combusted in heat-treatment process.

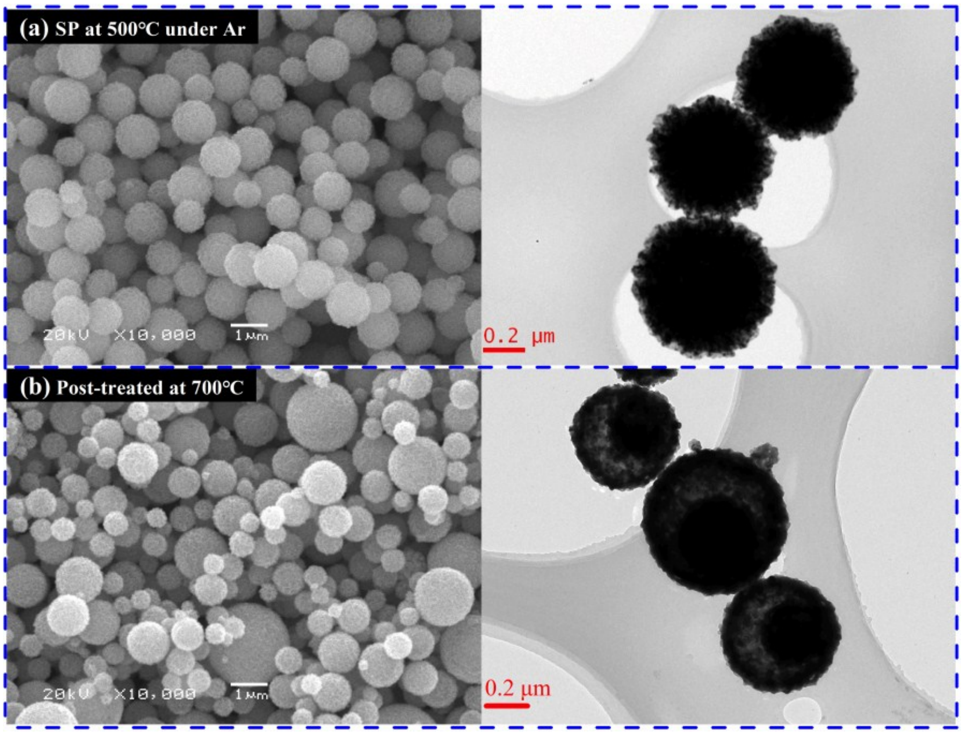

Figure S3 Morphology of the powder particles directly synthesized by SP at 500 °C under Ar atmosphere and the as-prepared particles after heat-treated at 700°C for 30 minutes in air: a) synthesized by SP at 500 °C under Ar, b) heat-treated at 700°C.

To demonstrate the formation mechanism of multishell yolk-shell structure, another similar yolk-shell nickel-cobalt oxide microspheres were synthesized by two-step fabrication technique. The precursor particles directly prepared by SP with 5g PVP at 500°C under Ar atmosphere show a stuffed spherical morphology (Figure S3a) with neither void nor core structure inside. Interestingly, the powders heat-treated at 700°C for 30 minutes in air exhibit yolk-shell structure (Figure S3b) which is similar to the samples directly prepared by SP with PVP at 700°C under O_2 atmosphere (Figure 1).

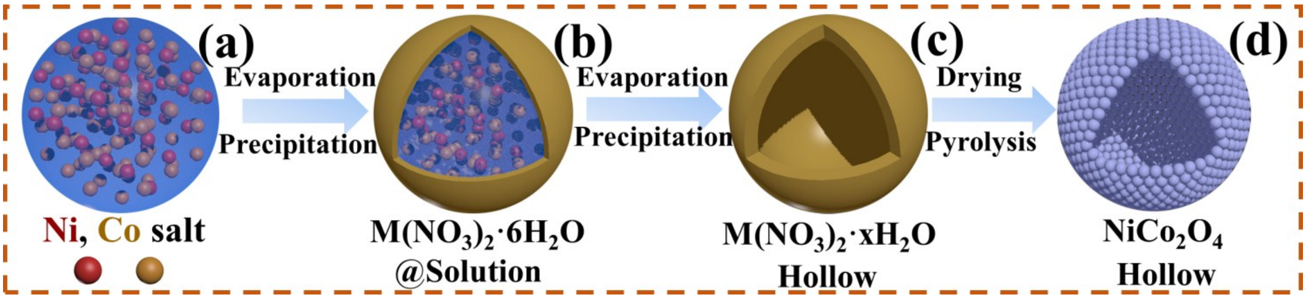

Scheme S1 Formation mechanism of single-shelled hollow Nickel-cobalt oxide microspheres.

The formation mechanism of single-shelled hollow nickel-cobalt oxide microspheres prepared by one-pot SP method without PVP is illustrated in Scheme S1. Firstly, the Ni/Co nitrates solution is atomized to micron-size (≤10μm) spherical droplets and fed into a 700 °C tubular furnace reactor (Figure S1) by oxygen as carrier gas (Scheme S1a). Then, solvent quickly evaporates from the surface of the droplet and the Ni/Co nitrates are gradually concentrated within the droplet. When the superficial solutes concentration exceed the saturation concentration, the salts start to deposit on the surface and form a $M(NO_3)_2.6H_2O$ (M = Co/Ni) shell (Scheme S1b). When the evaporation of the solvent is completed, the $M(NO_3)_2.6H_2O$ will gradually lose the crystal water and form a single-shelled hollow $M(NO_3)_2.xH_2O$ structure (Scheme S1c). The further drying, pyrolysis, and crystallization lead to forming hollow nickel-cobalt oxide microsphere (Scheme S1d).

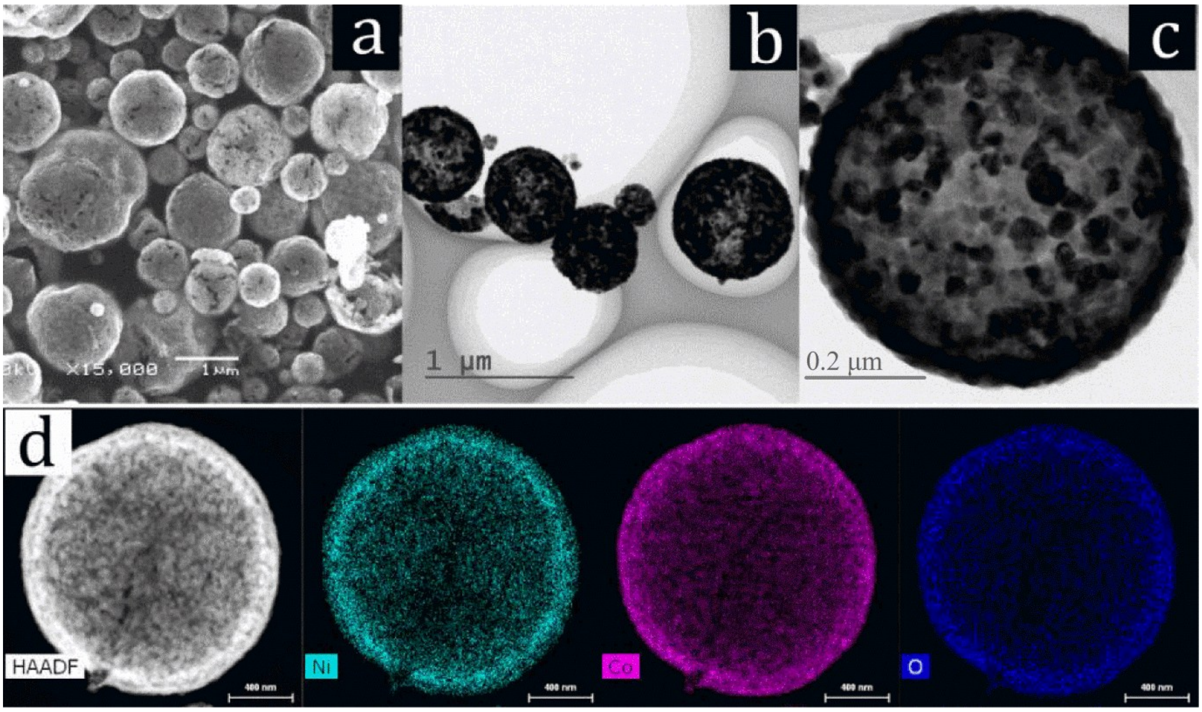

Figure S4 Morphology and elemental-mapping of the hollow Nickel-cobalt oxide microspheres: a) SEM image; b, c) TEM images, and d) elemental-mapping images.

As shown in Figure S4, the powder particles, which are prepared under the same preparation condition just without PVP, clearly exhibit a single-shelled hollow structure. The dot-mapping images for the Ni, Co, and O contents of the hollow structured Nickel-cobalt oxide microspheres, as shown in Figure S4d, indicate that all of these elements were uniformly distributed in the single-shelled hollow structure.

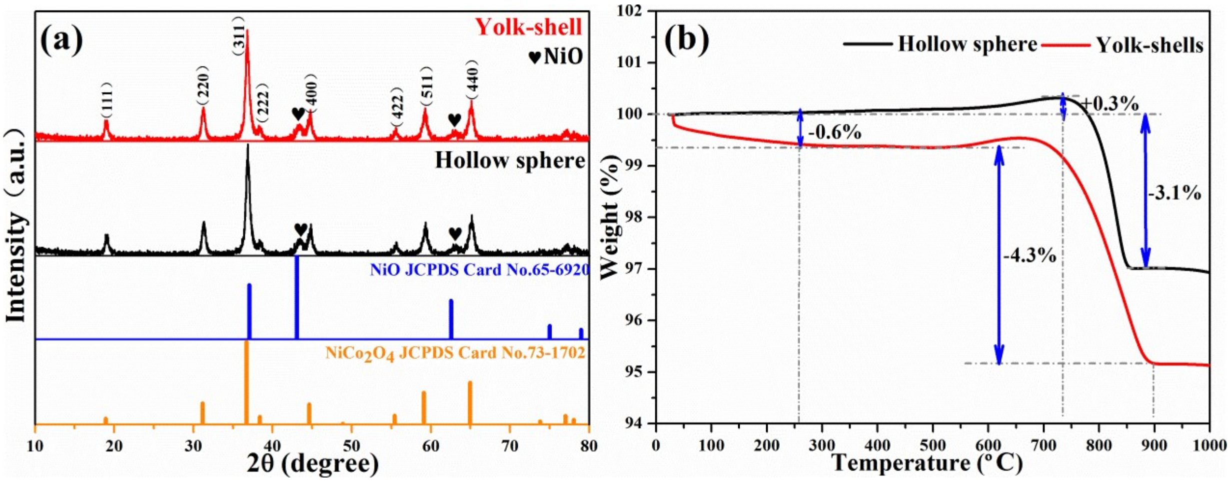

Figure S5 XRD patterns and TG curves of the yolk-shell structured microspheres and hollow microspheres: a) XRD patterns, b) TG curves.

The XRD pattern of the hollow nickel-cobalt oxide microspheres prepared by SP without PVP at 700°C demonstrate the sample have the same crystal structure as multishell yolk-shell microspheres, consisting of major $NiCo_2O_4$ with a minor NiO phase.

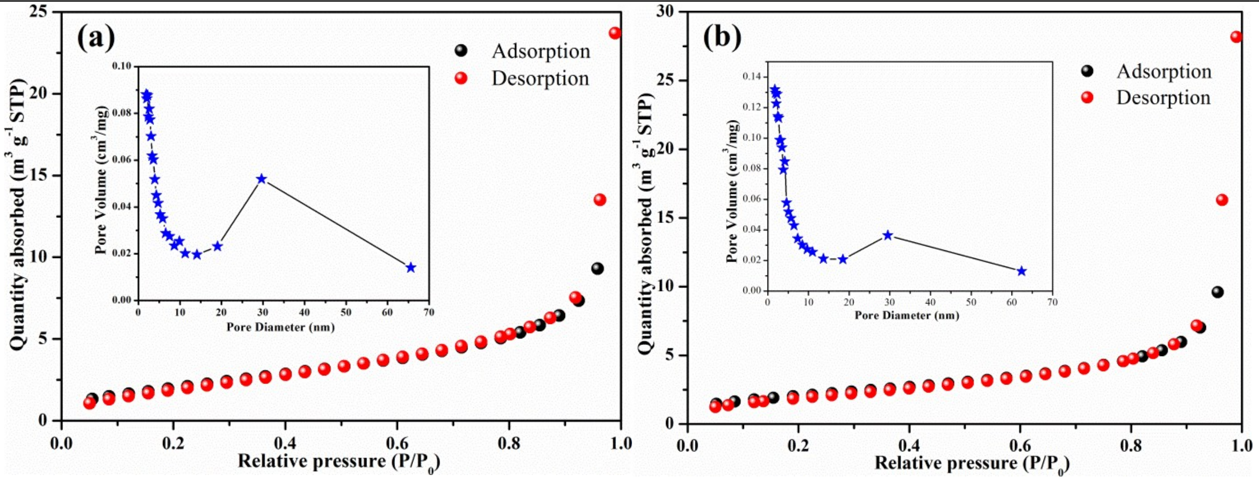

Figure S6 N_2 adsorption-desorption isotherms and pore size distribution of the multishell yolk-shell structured microspheres and hollow microspheres: a) multishell yolk-shell structured microspheres, b) hollow microspheres.

Table S1 BET surface area, Pore volume, and BJH average pore diameter of the samples.

Samples	BET surface area (m^2/g)	Pore volume(cm^3/g)	BJH average pore diameter(nm)
Multishell Yolk-shell	7.87	0.037	18.6
Hollow	7.50	0.044	23.2

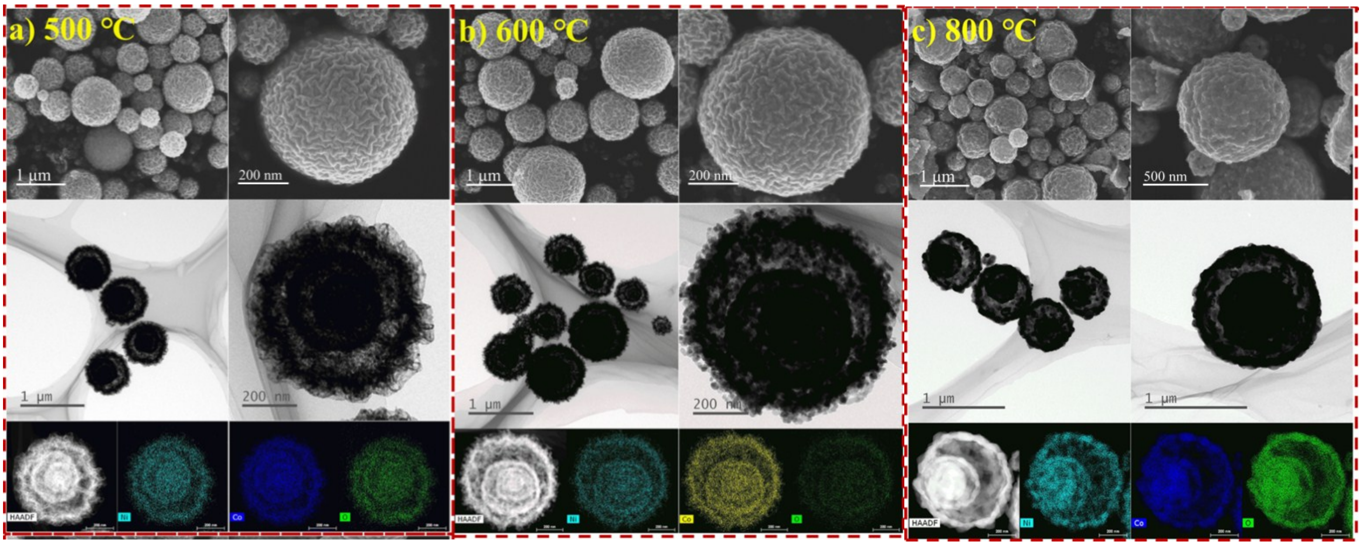

Figure S7 Morphologies and elemental-mapping images of the particles prepared with 5g PVP at the different temperatures: a) 500, b) 600, and c) 800°C.

In order to investigate the impact of preparation temperature, the particles are prepared with 5g PVP at the different preparation temperatures of 500, 600, 700 and 800°C, respectively. As shown in Fig. S7, regardless of the preparation temperatures, all of sample exhibit a yolk-shell structure. The particles prepared at the temperatures of 500 and 600°C have the same structure as the particles prepared at 700°C with triple-shelled yolk-shell structure. The particles prepared at 800°C also have yolk-shell structure with two shells. This set of experiment results indicates that this method is a powerful technique that can be applied in a wide temperature range.

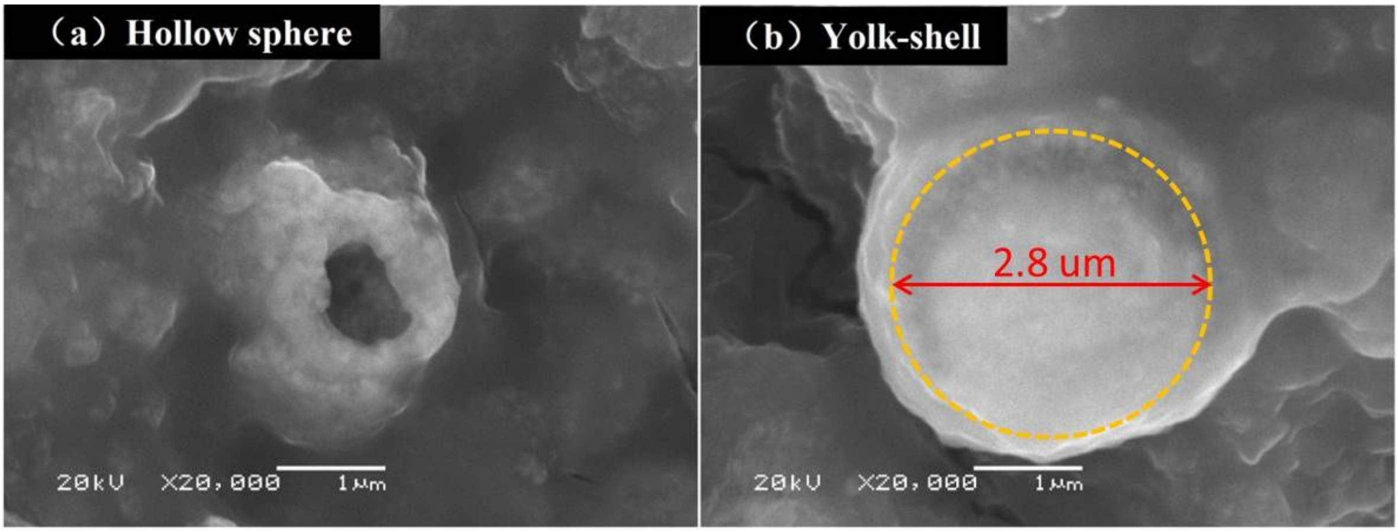

Figure S8 Morphologies of the yolk-shell structured and hollow structured Nickel-cobalt oxide microspheres obtained after 100 cycles at a current density of 400 mA g^{-1}: a) hollow microspheres, b) multishell yolk-shell microspheres.

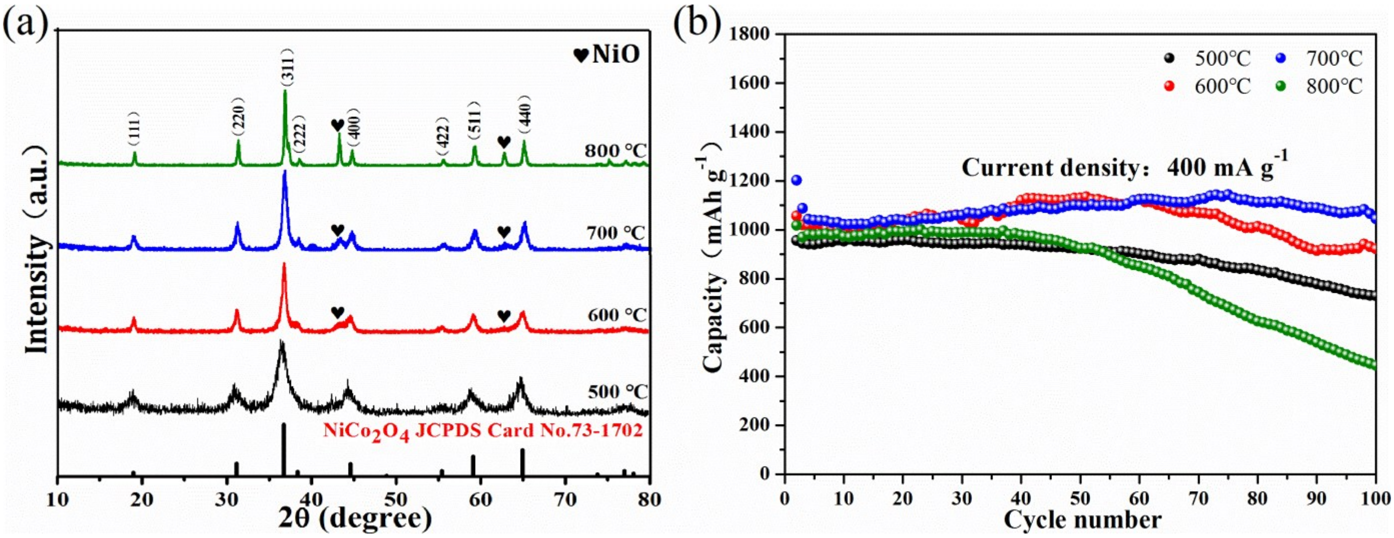

Figure S9 XRD patterns and cycle performances of the four samples prepared at different temperature: a) XRD patterns, b) cycle performance

As shown in Figure S9a, all as-prepared samples exhibit sharp crystalline peaks and the intensity of peaks increase with the rising temperatures. As reported in previous literatures, $NiCo_2O_4$ is believed to decompose when the synthesis temperature is between 500 and 800 °C [1, 2]. In this work, it is clear that only the sample prepared at 500 °C can be precisely indexed to $NiCo_2O_4$ (JCPDS no. 73-1702). The all other samples consist largely of $NiCo_2O_4$ with a minor NiO (JCPDS no. 65-2901) phase. In addition, the characteristic peaks intensity of NiO increase obviously as rising the preparation temperatures, signifying that an increased amount of $NiCo_2O_4$ have decomposed. As shown in Figure S9b, the 100th reversible capacity of the samples increased with the temperature increased from 500 to 700 °C. This result means that an appropriate amount of NiO phase can contribute to stabilizing the structure of the material and improving the recycling properties. The sample prepared at 800 °C exhibits the worst cycle performance. In total, the sample prepared at 700 °C shows the best cycle performance.

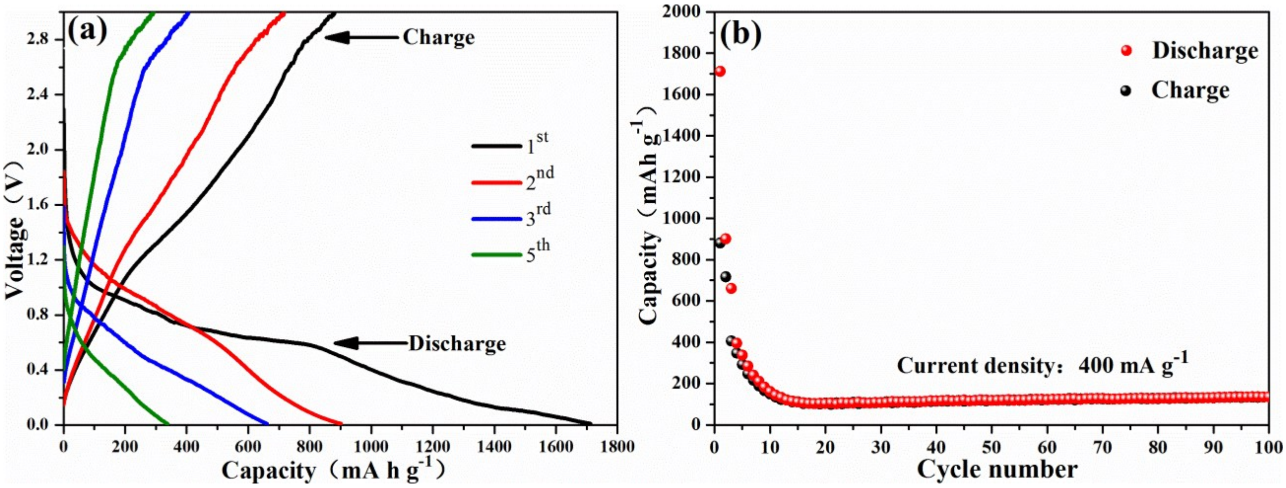

Figure S10 Electrochemical performance of the sample without carbon removal: a) charge and discharge curves of 1st, 2nd, 3rd and 5th cycles, b) cycling performance.

As shown in Figure S10a, the initial discharge curve of the sample without carbon removal has only one obvious plateau at about 0.75 V, which is corresponded to the reduction reactions of NiO/CoO_x to metallic Ni/Co and generation of amorphous Li_2O phases. The first cycle discharge capacity of the sample is 1717 mAh g^{-1}, and the parallel charge capacity is 887 mAh g^{-1}. However, as shown in Figure S10b, the sample without carbon removal shows fast capacity decay at a current density of 0.4 A g^{-1}.

References

1. B. Cui, H. Lin, J.-B. Li, X. Li, J. Yang and J. Tao, *Advanced Functional Materials*, 2008, **18**, 1440-1447.
2. S. H. Choi, S. K. Park, J.-K. Lee and Y. C. Kang, *Journal of Power Sources*, 2015, **284**, 481-488.
3. E. Umeshbabu, G. Rajeshkhanna and G. R. Rao, *International Journal of Hydrogen Energy*, 2014, **39**, 15627-15638.
4. K. M. Jeon, J. S. Cho and Y. C. Kang, *Journal of Power Sources*, 2015, **295**, 9-15.
5. S. M. Lee, S. H. Choi and Y. C. Kang, *Chemistry*, 2014, **20**, 15203-15207.